

Selectivity Reversal in Oxidative Dehydrogenation of Ethane with CO₂ on CaO–NiO/Al₂O₃ Catalysts

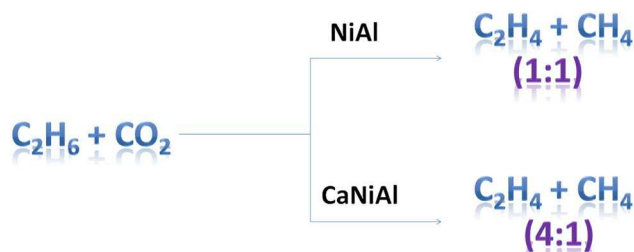
T. V. Sagar¹ · M. Surendar¹ · D. Padmakar¹ · G. Parameswaram¹ · N. Lingaiah¹ · K. S. Rama Rao¹ · I. A. K. Reddy² · C. Sumana³ · P. S. Sai Prasad¹

Received: 17 March 2016 / Accepted: 27 October 2016
© Springer Science+Business Media New York 2016

Abstract CaO–NiO/Al₂O₃ catalysts were prepared by wet impregnation method, keeping the NiO composition constant at 25 wt.% and varying the CaO composition in the range 6–12 wt.%. The catalysts were evaluated for oxidative dehydrogenation (ODH) of ethane with CO₂ at atmospheric pressure and in the temperature range of 600–700 °C. The physicochemical characterization of the catalysts was carried out using X-ray diffraction (XRD), BET surface area, Temperature programmed reduction (TPR), Temperature programmed desorption of CO₂ (CO₂-TPD), H₂ chemisorption, Carbon analysis and Fourier transform infrared (FT-IR) spectroscopy. NiO/Al₂O₃ showed higher ethane and carbon dioxide conversions, but with lower ethene selectivity. The addition of CaO in NiO/Al₂O₃ reversed the course of reaction leading to high selectivity to ethene, although at reduced conversions. 9 wt.% CaO containing NiO/Al₂O₃ emerged as the most promising catalyst giving the highest yield of ethene. CaO addition increased the basicity and the coke resistance. The shift in selectivity with CaO addition is explained in terms of more probability for reverse water gas shift reaction on a basic site rather than the hydrocracking reaction on the acidic sites of

Ni/Al₂O₃. The 9 wt.% CaO-25% NiO/Al₂O₃ catalysts were also prepared by changing the sequence of impregnation and by adopting simultaneous deposition of the two oxides on Al₂O₃. The activity of these catalysts was compared to identify the best method of catalyst preparation.

Graphical Abstract Ca promotion of NiAl modifies the surface basic property increasing ethene/methane selectivity ratio from 1 to 4, and enhances coke resistance.



Keywords Ethane to ethene · Carbon dioxide · ODH of ethane · Ca doping

Electronic Supplementary Material The online version of this article (doi:10.1007/s10562-016-1899-y) contains supplementary material, which is available to authorized users.

✉ P. S. Sai Prasad
saiprasad@iict.res.in

¹ I&PC Division, CSIR-Indian Institute of Chemical Technology (CSIR-IICT), Hyderabad 500 007, India

² Chemistry Department, National Institute of Technology (NITW), Warangal 506004, India

³ Chem. Engg. Division, CSIR-Indian Institute of Chemical Technology (CSIR-IICT), Hyderabad 500 007, India

1 Introduction

Ethene is one of the largest-volume petrochemical monomer used in the production of plastics, fibres and other organic chemicals [1, 2]. The global production of ethene touched 160 million tonnes in 2015, increasing at a rate of 4% per annum [3]. Commercially, ethene is produced by steam cracking of higher alkanes or naphtha, a highly endothermic and energy intensive reaction [4–6]. Catalytic oxidative dehydrogenation (ODH) of ethane to ethene has emerged as an alternative to steam cracking due to its many

advantages like overcoming the equilibrium limitation and a considerable reduction in energy demand [7]. The presence of O₂ as a co-reactant decreases the endothermicity of the cracking reaction, but leads to the production of over oxidation products like CO_x. In order to obviate this disadvantage, the mild oxidant CO₂ is preferred to increase the selectivity and hence the yield of ethene [8–10]. The utilization of CO₂ for ODH also helps to mitigate the global warming problem [11]. However, catalyst deactivation due to coking during the reaction is realized in the ODH of ethane even with CO₂ as the oxidant [12, 13]. Thus, any catalyst development activity on ODH of ethane should address coke formation during the reaction, apart from achieving high activity and selectivity.

Ni based catalysts have been extensively used for the ODH of ethane [14, 15]. Literature reveals that in the case of Ni, the free availability of electrophilic O[−] species on its surface decreases the ethene selectivity [16–18]. In order to obviate this disadvantage the catalysts are modified with Al ions. Modulation of the chemical properties of the highly reactive O[−] species around Ni results in the formation of high selective sites useful for the ODH of ethane [19, 20]. Smolakova et al. have also substantiated this claim showing higher selectivity on Ni-Al hydrotalcites [21]. Of late, there have been reports highlighting the advantages of Ca in the ODH catalysts. For example, Ca ions, in solid solution with CeO₂, have been shown to improve the efficiency of CO₂ used as a soft oxidant [22]. Hence, it is prudent to study the influence of Ca addition to Ni-Al catalysts on ethene selectivity.

In this study, an attempt has been made to delineate the influence of CaO addition on ethane conversion and ethene yield of NiO/Al₂O₃ catalysts during the ODH of ethane with CO₂. Identifying the optimum composition of CaO in the catalyst to get maximum yield of ethene, and the factors involved in achieving this, are the main objectives of this work. Besides, studying the effect of the addition of this basic species on the extent of coke formation during the reaction is yet another objective.

2 Experimental

2.1 Material Synthesis

Heracleous et al. in a study on Ni based catalysts for ODH of ethane, reported an optimum composition of 25 wt.% for NiO [15]. Based on this report, NiO/Al₂O₃ with a constant NiO composition of 25 wt.% in the finished catalyst was first prepared by the impregnation of commercial γ -Al₂O₃ (M/s. Sud Chemie, S.A.: 201 m²/g) with the required quantity of an aqueous solution of Ni(NO₃)₂·6H₂O (M/s. SD Fine, India, A.R. grade). After evaporating the excess solution on a water bath, the solid was dried in an air oven at

120 °C overnight and finally calcined in air at 750 °C for 4 h. It is denoted as NiAl in the present text. The NiAl thus prepared was then impregnated with required quantities of aqueous Ca(NO₃)₂·4H₂O (M/s. SD Fine, India, A.R. grade), such that the final catalysts contained 6, 9 and 12 wt.% of CaO (represented as 6CaNiAl, 9CaNiAl and 12CaNiAl, respectively). A control catalyst with 9 wt.% CaO on Al₂O₃ was prepared by wet impregnation and is denoted as 9CaAl. Two more catalysts were prepared, one by depositing CaO first followed by NiO and the other by a simultaneous deposition of CaO and NiO on Al₂O₃ support. Evaporation, drying and calcination steps for all the Ca containing catalysts were similar to that of NiAl catalyst.

2.2 Catalyst Characterization

BET surface area of the catalysts was determined by N₂ adsorption at liquid nitrogen temperature on a SMART SORB 92/93 instrument (M/s. SMART Instruments, India). Prior to the measurement, degasification of samples was carried out at 150 °C for 2 h. XRD patterns of the catalysts were obtained on an Ultima-IV diffractometer (M/s. Rigaku Corporation, Japan) using nickel-filtered Cu K α radiation ($\lambda = 1.54 \text{ \AA}$). The measurements were recorded in steps of 0.045° with a count time of 0.5 s and in the 2 θ range of 10–80°. Identification of the crystalline phases was carried out with the help of JCPDS files. TPR studies were performed using a home-made apparatus. Catalyst sample (50 mg) taken in a quartz reactor, was first treated in argon flow at 300 °C for 2 h. Then the reduction preceded under 10% H₂/Ar gas mixture at a flow rate of 30 ml/min and a heating rate of 5 °C/min from 25 to 800 °C, keeping the temperature constant for 1 h after reaching the final temperature. The hydrogen consumption was monitored using a TCD equipped gas chromatograph (Varian, 8301). H₂ chemisorption experiments were conducted in a quartz reactor system with 50 mg of catalyst. The catalyst was first reduced under H₂/Ar gas mixture at a flow rate of 30 ml/min at 600 °C for 1 h, and then the reactor was cooled to room temperature. A series of H₂ pulses were given until the saturation point was reached. The hydrogen consumption in the pulses was estimated gas chromatographically. CO₂-TPD was carried out on a BELCAT II (M/s. BEL Japan, Inc.) apparatus using a TCD detector. In a typical experiment about 50 mg of the oven dried sample was taken in a quartz tube. The sample was first pre-treated at 300 °C for 1 h in pure helium (99.9%, 50 ml/min) and then saturated with CO₂ (10% CO₂–90% He mixture gas) at 80 °C, passed at a flow rate of 50 ml/min for 1 h. After flushing with He at the same temperature to remove physisorbed CO₂, the TPD analysis was carried out from ambient temperature to 800 °C at a heating rate of 10 °C/min. The amount of CO₂ evolved was calculated from the peak area of the already calibrated TCD signal. FT-IR spectra of the used catalysts were recorded on a Biorad-Excalibur series (USA)

spectrometer using the KBr disc method. Enough caution was exercised to see that the samples were not exposed to external atmosphere. The coke content in the spent catalysts was determined on a CHNS analyzer (M/s. ElementaV, Germany).

2.3 Activity Test

The evaluation of the catalysts was performed in a fixed-bed stainless steel reactor passing a mixture of He/C₂H₆/CO₂ at a ratio of 30/20/10, at atmospheric pressure. The activity tests were carried out using 0.5 g of catalyst diluted with the same amount of ceramic beads and placed between two quartz wool plugs in the reactor. Prior to the activity measurements, the sample was pretreated in He flowing at 30 ml/min at 500 °C for 4 h. The activity tests were conducted in the temperature range of 600–700 °C. The outlet gases were analyzed by an online Nucon 5765 gas chromatograph equipped with a Porapak-Q column, using He gas as carrier and a TCD detector. After attaining the required temperature and reaching the steady-state over a period of 1 h, the product analysis was duplicated and the average value considered. The accuracy was within the error margin of ±3%.

The following formulae were used:

$$\text{Conversion of } i = \frac{\text{Moles of } i(\text{in}) - \text{Moles of } i(\text{out})}{\text{Moles of } i(\text{in})} \times 100\%,$$

where i = reactant C₂H₆, CO₂

$$\text{Selectivity of } j = \frac{j}{\sum j} \times 100\%,$$

where j = product species C₂H₄, CH₄

$$\text{Yield} = (\text{Conversion} \times \text{Selectivity}) \times \left(\frac{1}{100}\right)\%.$$

3 Results and Discussions

3.1 Specific Surface Area

Table 1 displays the specific surface area values of the catalysts which trace a decreasing trend after the addition of CaO. 9CaAl shows a surface area of 101.1 m²g⁻¹. This

Table 1 Specific surface area, Ni dispersion and particle size of the fresh and carbon content of the used catalysts

Catalysts	Specific surface area (m ² /g)	Dispersion (%)	Particle size (nm)	Basicity (m mol/g)	Extent of coking (wt.%) ^a
NiAl	114.5	4.1	24	0.184	2.89
6CaNiAl	101.9	3.4	29	0.618	2.07
9CaNiAl	53.3	4.8	20	0.866	0.53
12CaNiAl	73.6	3.7	26	0.711	0.78

^aCoke formation expressed in terms of the C content of the used catalyst

trend is due to possible pore filling, as also observed by Dias et al. [23]. Catalysts with low surface area are found to be advantageous in terms of controlling the side reactions [24].

3.2 X-ray Diffraction Studies

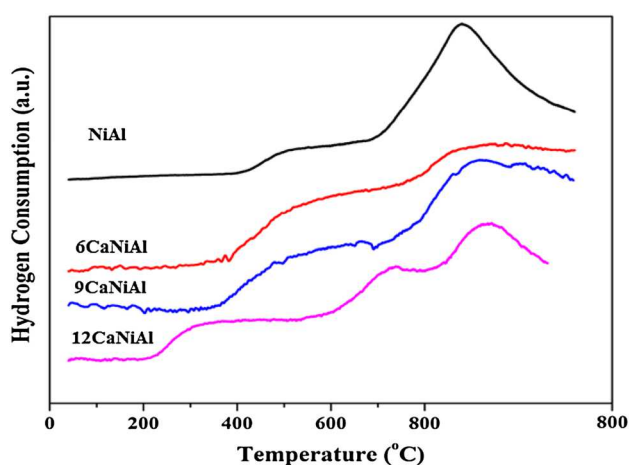
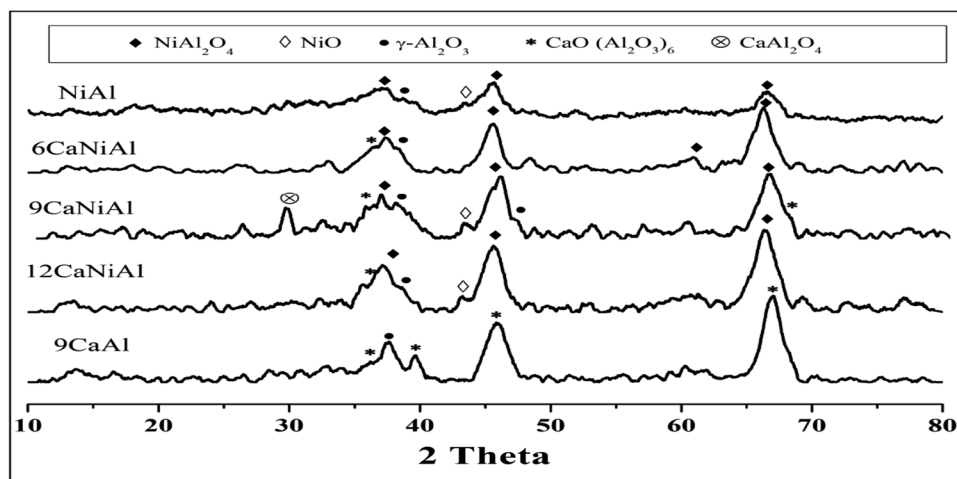
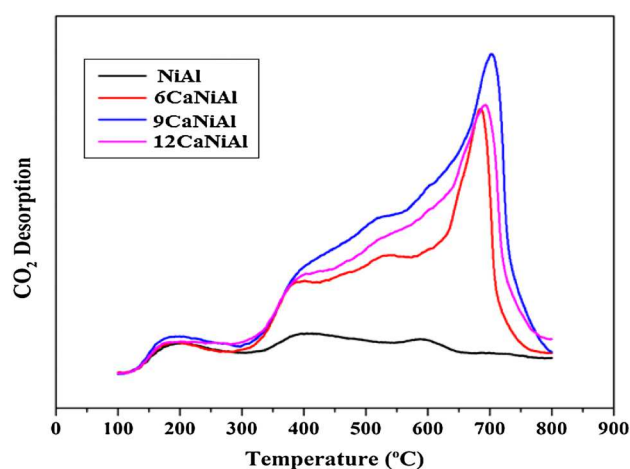
Figure 1 shows the XRD patterns of the fresh catalysts. NiAl displays broad diffraction peaks at 2θ values of 37.2, 45.6 and 66.6° corresponding to NiAl₂O₄ (JCPDF:78-1601) and weak peaks due to NiO. However, the presence of γ-Al₂O₃ (JCPDF:29-0063) cannot be excluded as its peak positions are very close to that of the spinel. The agglomerated CaO(Al₂O₃)₆ phase is seen with peaks at 37.6, 46.0 and 67.1° (JCPDF-76-0665) in the patterns of CaO containing catalysts; 9CaAl showing its predominant formation. In the presence of CaO the samples show noticeable levels of NiO. The basically broad and low intense peaks in the patterns indicate high interactions of active metal oxide species with the support giving the possibility for the formation of spinel structures.

3.3 Temperature Programmed Reduction

The TPR patterns shown in Fig. 2 distinguish two major peaks appearing at low (500 °C) and high (800 °C) temperatures, respectively. Both the peaks represent the Ni²⁺ to Ni⁰ reduction; the low temperature peak due to the reduction of NiO with medium oxide-support interaction and the high temperature one due to the reduction of the Ni phase in NiAl₂O₄. With the addition of CaO the intensity of the high temperature peak decreases, revealing that the reduction of NiO in the spinel is considerably decreased. In the case of high CaO containing catalyst (12CaNiAl) a new peak appears at 280 °C, which may be due to the reduction of free NiO on the surface of CaO agglomerated on Al₂O₃, as evidenced by the XRD studies and also reported in the literature [23–27].

3.4 CO₂-Temperature Programmed Desorption

CO₂-TPD study reveals the acid/base nature of the catalysts. The patterns obtained on the catalysts are shown in Fig. 3. The desorption bands with peaks appearing at about

Fig. 1 XRD patterns of calcined catalysts**Fig. 2** TPR patterns of calcined catalysts**Fig. 3** CO₂-TPD patterns of calcined catalysts

200, 400–500 and 675–700 °C on the CaO containing catalysts correspond to the weak, medium and strong basic sites [28]. The intensity of the high temperature desorption peak is seen increasing upto 9CaNiAl due to increase in the strong basic sites on the surface of the catalysts. Further addition of CaO to 12 wt.% (12CaNiAl) has shown a decreasing trend. Though NiAl has shown a similar pattern, the intensities of the peaks are much lower than the CaO containing catalysts.

3.5 H₂ Chemisorption

Studying Ni-Nb-O mixed oxide catalysts, Heracleous and Lemonidou [29] observed segregation phenomena between Nb₂O₅ and NiO phases for Nb/Ni atomic ratio >0.176. The same authors also identified a correlation between activity of the catalysts and surface exposed Ni content. Thus, metal oxide dispersion is a crucial factor in the ODH performance

of the catalysts. Therefore, the metal dispersion and particle size of Ni in the catalysts were determined to reflect the metal oxide content on the surface and the values are reported in Table 1. Ni dispersion on NiAl is obtained as 4.1% with the corresponding particle size of 24 nm. CaO promotion has not varied the Ni dispersion (3.4–4.8%) and the Ni particle size (20–29 nm) much. It appears that CaO has covered the surface sites. However, in numerical terms the dispersion is the highest and the corresponding particle size is the lowest in 9CaNiAl.

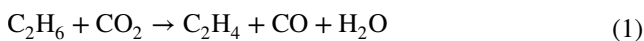
3.6 Catalytic Activity

The activity results of the catalysts are reported in Table 2. At a reaction temperature of 700 °C, NiAl shows higher conversion values for both ethane and carbon dioxide (26.2 and 45.1%, respectively) compared to the CaO containing catalysts. However, its ethene selectivity is much lower (52%).

CaO addition has led to drop in conversion of the reactants. What is interesting is the attainment of high selectivity towards ethene. 9CaNiAl has appeared to be promising in terms of ethane conversion and ethene selectivity among the CaO containing catalysts. This catalyst has given the maximum ethene yield of 14.9%.

The effect of reaction temperature on ethene selectivity and yield obtained on 9CaNiAl catalyst is shown in Fig. 4. Increase in reaction temperature increases the conversion. Higher CO₂ conversions are realised at high reaction temperatures, indicating that activation of this reactant requires higher temperatures. ODH of ethane is a complicated reaction involving simultaneous occurrence of several reactions, as shown below. While Reactions 1 and 2 increase ethylene selectivity, Reactions 3 and 4 are deleterious as they lead to the production of unwanted product, methane. Under the reaction conditions the Reverse Water Gas Shift (Reaction 5) can also occur. Reaction 6 is a deactivation reaction resulting in coking on the surface of the catalysts. Ultimately, the product stream contains ethene, water vapour, carbon monoxide and unreacted ethane and carbon dioxide.

Oxidative dehydrogenation.



Dehydrogenation of ethane.



Hydrocracking of ethane.



CO₂ methanation.



Reverse Water Gas Shift (RWGS) Reaction.



Carbon formation.



In the case of NiAl catalyst, apart from the ODH reaction (Reaction 1) giving ethene, the facile ethane conversion may be due to the predominance of dehydrogenation (Reaction 2) and hydrocracking (Reaction 3) of ethane occurring on the Ni sites. The higher conversion of CO₂

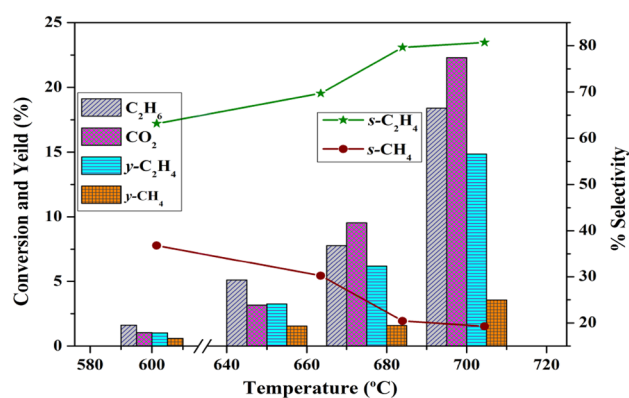


Fig. 4 Temperature study of 9CaNiAl catalyst

observed on this catalyst compared to the others indicates that CO₂ methanation (Reaction 4) is also feasible. Even though the conversion values are high on this catalyst, its methane selectivity is almost equal to that of ethene (Table 2), which is not very advantageous for the selective synthesis of the alkene. Compared with this catalyst, the CaO containing catalysts show very high ethene/methane ratio (4:1) in the product which is significant. Particularly, the overall yield of ethene is the highest in the case of 9CaNiAl catalyst. Very recently Myint et al. [30] have reported that the reaction pathway can also depend on the nature of catalyst. Whereas CoMo/CeO₂ and NiMo/CeO₂ followed the reforming pathway, FeNi/CeO₂ followed the oxidative dehydrogenation pathway to produce ethylene.

NiAl exhibits very low basicity (Table 1), as revealed by its CO₂-TPD profile. Its ethene selectivity is also low. On the other hand, the highest selectivity to ethene is obtained on the most basic 9CaNiAl catalyst. Thus, basicity appears to be a reason for obtaining high ethene yield. The conversion-yield and conversion-basicity relationships are shown in Fig. 5. The parallelism between the two curves indicates that yield is proportional to basicity. Valenzuela et al. [31] have observed increase of oxygen-ion mobility and the surface basicity of the catalyst in the presence of Ca in CeO₂. Xin et al. [32] have characterized the structure and surface acidity/basicity of CeO₂/γ-Al₂O₃ catalysts and reported that surface acidity decreases while surface basicity increases after the addition of CeO₂ to γ-Al₂O₃. The selectivity to

Table 2 The performance of the ODH catalysts at 700 °C

Catalysts	Conversion (%)		Selectivity (%)		Yield (%)	
	C ₂ H ₆	CO ₂	C ₂ H ₄	CH ₄	C ₂ H ₄	CH ₄
NiAl	26.2	45.1	52.5	47.5	13.7	12.5
6CaNiAl	17.1	31.9	63.9	36.1	10.9	6.2
9CaNiAl	18.4	22.3	80.7	19.3	14.9	3.6
12CaNiAl	12.5	18.9	80.2	19.8	10.0	2.5

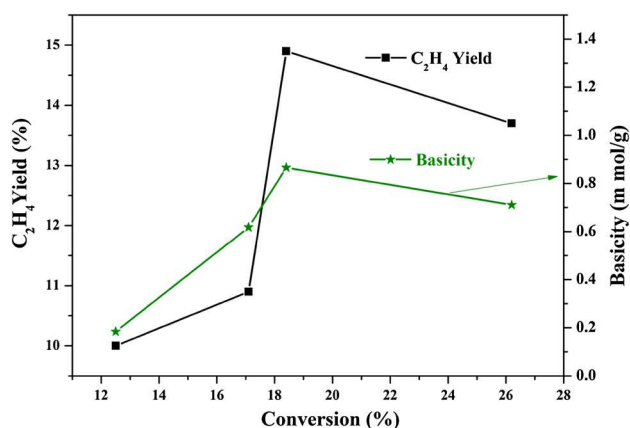


Fig. 5 Variation of ethene yield and catalyst basicity with ethane conversion

ethene is shown to increase for all the CeO_2 , $\gamma\text{-Al}_2\text{O}_3$ and $\text{CeO}_2/\gamma\text{-Al}_2\text{O}_3$ catalysts. In order to further substantiate the claim that basicity is responsible for ethene selectivity and in turn its yield, the control catalyst, 9CaAl (without Ni) was also tested for the ODH reaction. At 700°C , the catalyst has shown 13% ethane conversion with 84% selectivity to ethene (ethene yield: 11%), reiterating the fact that increase in basicity increases the ethene selectivity.

Increased yield of ethene with increased basicity needs to be understood. One probability is the occurrence of basic site activated RWGS reaction (Reaction 5) that consumes the hydrogen produced during the decomposition of ethane pushing the reaction forward. It is known that CO_2 enhances the equilibrium conversion of C_2H_4 formation via dehydrogenation of C_2H_6 and reacts with the carbon deposited on the surface. Both the functions are positive in nature. The former stabilizes the activity and the latter prolongs the catalyst life, as reported by Li et al. [33].

CO is one of the products of RWGS reaction. However, it was not detected in sufficient quantities in the product in the present work. The absence of CO can be explained by considering the methanation reaction (Reaction 4). Fecheté and Vedrine, in a recent review, have proposed different mechanisms for CO_2 methanation. In one of the mechanisms, CO_2 is first converted to CO and then hydrogenated to methane [34]. Taking this into consideration we may propose that in the presence of hydrogen not only the CO produced during methanation but also that produced from RWGS reaction would have been converted to methane.

An examination of the performance stability of 9CaNiAl catalyst by continuing the evaluation for 300 min at 700°C , reveals that the catalyst has reasonable stability till 210 min. The ethane conversion is seen to increase from 21.9% after 210 min to 23.2% after 300 min, whereas the ethene yield decreased from 12.8 to 12.0% during the same period.

Table 3 compares the activity of 9CaNiAl catalyst with that of the catalysts prepared by changing the method of preparation. It can be seen that in the case of catalyst prepared by depositing CaO first and NiO later on Al_2O_3 (NiCaAl) and the catalyst prepared by simultaneous deposition of CaO and NiO on Al_2O_3 [(Ni + Ca)Al], the ethane conversion is higher than that of the 9CaNiAl catalyst. However, there is a distinct decrease in the selectivity towards ethene. Whereas 9CaNiAl shows high ethene selectivity, the other catalysts are selective towards methane formation. Therefore, the sequence of depositing NiO first followed by CaO on Al_2O_3 appears to be the best method for the catalyst preparation.

3.7 Effect of CO_2 Partial Pressure on the Activity of the Catalysts

Experiments were conducted by varying CO_2 partial pressure in the feed and the results are included in Table 4. It can be observed that the CO_2 conversion increases exponentially with its partial pressure, particularly at high reaction temperature. The ethane conversion initially increases and then decreases. The effect of CO_2 partial pressure is particularly felt on the ethene selectivity which shows a tremendous decrease from 80 to 20%. Methane formation on the other hand increases with increase in CO_2 concentration in the feed. This is an interesting observation. The competitive adsorption of CO_2 in preference to ethane has decreased ethane conversion (Table 4) with simultaneous increase in methanation of carbon dioxide.

3.8 Estimation of the Thermodynamic Equilibrium Composition

The thermodynamic equilibrium composition of the product was calculated for the input gas conditions (molar ratio: $\text{C}_2\text{H}_6/\text{CO}_2/\text{He} = 2:1:3$) using HSC Chemistry Version 9.0 (Outotec Technologies, USA). The variation in product composition against temperature is depicted in Figs. S1 and S2. Preliminary results have indicated the presence of

Table 3 Activity comparison of different catalysts

Catalysts	Conversion C_2H_6 (%)	Selectivity C_2H_4 (%)	Selectivity CH_4 (%)	Extent of coking (%) ^a
9CaNiAl	18.4	80.4	19.3	0.53
NiCaAl	19.1	61.7	38.3	7.43
(Ni + Ca)Al	55.1	–	99.0	54.54

^aCoke formation expressed in terms of the C content of the used catalyst

Table 4 Effect of CO₂ concentration in the feed on the performance of the catalyst

Catalyst	Temperature (°C)	Conversion (%)		Selectivity (%)		Yield (%)	
		C ₂ H ₆	CO ₂	C ₂ H ₄	CH ₄	C ₂ H ₄	CH ₄
9CaNiAl (He:C ₂ H ₆ :CO ₂ 30:20:10)	600	1.6	1.0	63.2	36.8	1.0	0.6
	650	5.1	3.2	69.7	30.2	3.3	1.5
	675	7.8	9.5	79.6	20.4	6.2	1.6
	700	18.4	22.3	80.7	19.3	14.8	3.6
9CaNiAl (He:C ₂ H ₆ :CO ₂ 25:20:15)	600	2.3	2.1	0	100	0	2.1
	650	11.9	9.1	32.1	67.9	3.8	8.1
	675	19.3	17.6	58.4	41.6	11.4	8.0
	700	27.8	40.9	56.2	43.8	15.6	12.2
9CaNiAl (He:C ₂ H ₆ :CO ₂ 20:20:20)	600	2.1	7.3	0	100	0	2.5
	650	4.9	24.5	21.1	78.6	1.0	3.8
	675	10.5	47.9	18.3	81.6	1.9	8.5
	700	21.2	76.5	20.1	79.9	4.3	16.9

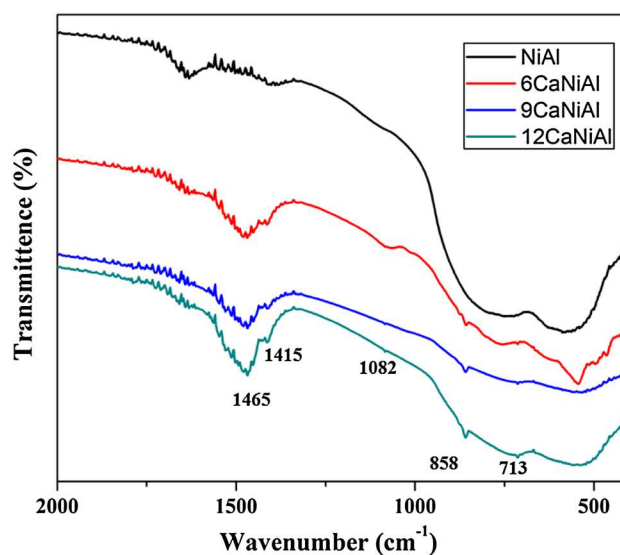
two temperature regions. In the low temperature (<400 °C) region ethane cracking to methane is found to be predominant, whereas in the high temperature region (>400 °C) ODH of ethane predominates. The inference is consistent with the experimental results. Between 600 and 700 °C, the composition of ethene is found to be considerable. However, the ethene/methane ratio varies in the presence of catalyst. Another interesting observation from the thermodynamic analysis is that when C(s) formation is taken into consideration coke formation appears to be predominating ethene and methane formation during the entire temperature region (Fig. S2). The very fact that the ethene selectivity is high on 9CaNiAl implies that the catalyst resists coke formation.

3.9 Coke Formation in used Catalysts

The coke accumulation was examined by determining the carbon composition of the used catalysts. The values are presented in Table 1. NiAl reveals a C content of 2.89% whereas the CaO containing catalysts show lower values indicating good coke resistance. According to Heracleous et al. [35] coking during the ODH reaction is due to C–C cracking of ethane on acidic centers like –OH and Al³⁺–O²⁻. These sites are normally neutralized by the addition of an alkaline earth species such as CaO. Particularly, the method of preparation adopting the sequence of depositing NiO first followed by CaO on Al₂O₃ is also advantageous compared to the other two methods in containing the coke formation, as seen from Table 3.

In order to confirm the formation of calcium carbonate in the present study, the used catalysts were examined by FTIR analysis. The spectra are reported in Fig. 6. The data obtained for the CaO containing samples reveal a broad absorption peak at 1455 cm⁻¹ and clear peaks at 1082, 858 and 713 cm⁻¹, which have been reported to be the common

characteristic features of the carbonate ion in calcium carbonate [36]. The bands at 1082 and 858 cm⁻¹ represent symmetric stretching and out-of-plane bending modes of the carbonate ion, respectively. The peak at 1082 cm⁻¹ usually observed in the spectrum is of aragonite-phase of calcium carbonate, whereas the one at 713 cm⁻¹ can be attributed to the in-plane bending mode of ions, which indicates a structural change in the calcium ions from the symmetry of the calcite phase. The band at 1455 cm⁻¹ represents the asymmetric stretching mode of carbonate ion. Thus, the Ca containing catalysts exhibit peaks due to calcium carbonate. Therefore, it could be expected that as the CaO content increases, the carbonate formation increases, in turn decreasing the coke formation. The data on the extent of coke formation on different catalysts reported in Table 1 supports this observation. When the reaction temperature is

**Fig. 6** FTIR spectra of used catalysts

low, the CaCO_3 formed covers the Ni sites. As a result the hydrocracking is limited, eventually decreasing the overall conversion. At high reaction temperatures the decomposition of CaCO_3 opens up the Ni sites on which the oxidative dehydrogenation takes place, again increasing the conversion.

4 Conclusions

NiAl offers high ethane and carbon dioxide conversions predominantly due to hydrocracking of ethane and methanation of carbon dioxide. Thus, it gives a gas product with its ethene/methane selectivity ratio almost equal to 1. The addition of CaO increases the basicity thereby increasing the selectivity towards ethene and bringing the ethene/methane ratio to 4. High selectivity and yield of ethene could be achieved on CaO -containing catalysts. Ca addition also decreases the coke formation. The sequence of addition of NiO and CaO to Al_2O_3 also influences the catalyst performance.

Acknowledgements The authors are thankful to DST and CSIR, New Delhi, for the financial assistance.

References

1. Grtner AC, Van Veen AC, Lercher JA (2013) *Chem Cat Chem* 5:3196
2. Zimmermann H, Walzl R (2000) *Ullmann's Encyclopedia of Industrial Chemistry*. Wiley-VCH, Weinheim
3. Ramesh Y, Thirumala Bai P, Hari Babu B, Lingaiah N, Rama Rao KS, Sai Prasad PS (2014) *Appl Petrochem Res* 4:247
4. Cavani F, Ballarini N, Cericola A (2007) *Catal Today* 127:113
5. Shi X, Ji S, Wang K, Li C (2008) *Energy Fuels* 22:3631
6. Leena K (2012) International survey of ethylene from steam crackers. *Oil Gas J* 110:85
7. Karamullaoglu G, Dogu T (2007) *Ind Eng Chem Res* 46:7079
8. Sri Hari Kumar A, Upendar K, Qiao A, Rao PSN, Lingaiah N, Kalevaru VN, Martin A, Sailu Ch, Sai Prasad PS (2013) *Catal Commun* 33:76
9. Ansari MB, Park SE (2012) *Energy Environ Sci* 5:9419
10. Shi X, Ji S, Wang K (2008) *Catal Lett* 125:331
11. Wang S, Zhu ZH (2004) *Energy Fuels* 18:1126
12. Blasco T, Lopez-Nieto JM (1997) *Appl Catal A* 157:117
13. Wang S, Murata K, Hayakawa T, Hamakawa S, Suzuki K (1999) *Chem Commun* 1:103
14. Schuurman Y, Ducarme V, Chen T, Li W, Mirodatos C, Martin GA (1997) *Appl Catal A Gen* 163:227
15. Heracleous E, Lee AF, Wilson K, Lemonidou AA (2005) *J Catal* 231:159
16. Skoufa Z, Xantri G, Heracleous E, Lemonidou AA (2014) *Appl Catal A Gen* 471:107
17. Heracleous E, Delimitis A, Nalbandian L, Lemonidou AA (2007) *Appl Catal A Gen* 325:220
18. Skoufa Z, Heracleous E, Lemonidou AA (2012) *Catal Today* 192:169
19. Zhang X, Gong Y, Yu G, Xie Y (2002) *J Mol Catal A Chem* 180:293
20. Solsona B, Ivars F, Dejoz A, Concepción P, Vázquez MI, López Nieto JM (2009) *Top Catal* 52:751
21. Smoláková L, Capek L, Botková S, Kovanda F, Bulánek R, Pouzar M (2011) *Top Catal* 54:1151
22. Wang Y, Takahashi Y, Ohtsuka Y (1999) *J Catal* 186:160
23. Dias JAC, Assaf JM (2003) *Catal Today* 85:59
24. Khalesi A, Hamid RA, Matin P (2008) *Ind Eng Chem Res* 47:5892
25. Vizcaíno AJ, Lindo M, Carrero A, Calles JA (2012) *Inter J Hydro Energy* 37:1985
26. Shia C, Zhangb P (2012) *Appl Catal B Environ* 115–116:190
27. Chen L, Lu Y, Hong Q, Lin J, Dautzenberg FM (2005) *Appl Catal A Gen* 292:295
28. Horiuchi T, Hidaka H, Fukui T, Kubo Y, Horio M, Suzuki K (1998) *Appl Catal* 167:195
29. Heracleous E, Lemonidou AA, (2006) *J Catal* 237:162
30. Myint M, Yan B, Wan J, Zhao S, Chen JG (2016) *J Catal* 343:168
31. Valenzuela RX, Bueno G, Corberan VC, Xu Y, Chen C (2000) *Catal Today* 61:43
32. Xin G, Shenghua H, Qing S, Jianyi S (2003) *J Nat Gas Chem* 12:119
33. Li YN, Guo XH, Zhou GD, He X, Bi YL, Li WX, Cheng TX, Wu TH, Zhen KJ (2005) *Pol J Chem* 79:1357
34. Fehete I, Jacques CV (2015) *Molecules* 20:5638
35. Heracleous E, Lemonidou AA (2006) *Catal Today* 112:23
36. Kamba AS, Ismail M, Ibrahim TA, Zakaria ZA (2013) *J Nanomater* 2013:398357